

ARTICLE OPEN

Unveiling noiseless clusters in complex quantum networks

Albert Cabot¹, Fernando Galve¹, Víctor M. Eguíluz¹, Konstantin Klemm¹, Sabrina Maniscalco² and Roberta Zambrini¹

The transport and storage of quantum information, excitations, and entanglement, within and across complex quantum networks is crucially affected by the presence of noise induced by their surroundings. Generally, the interaction with the environment deteriorates quantum properties initially present, thus limiting the efficiency of any quantum-enhanced protocol or phenomenon. This is of key relevance, for example, in the design of quantum communication networks and for understanding and controlling quantum harvesting on complex systems. Here, we show that complex quantum networks, such as random and small-world ones, can admit noiseless clusters for collective dissipation. We characterize these noiseless structures in connection to their topology addressing their abundance, extension, and configuration, as well as their robustness to noise and experimental imperfections. We show that the network degree variance controls the probability to find noiseless modes and that these are mostly spanning an even number of nodes, like breathers. For imperfections across the network, a family of quasi-noiseless modes is also identified shielded by noise up to times decreasing linearly with frequency inhomogeneities. Large noiseless components are shown to be more resilient to the presence of detuning than to differences in their coupling strengths. Finally, we investigate the emergence of both stationary and transient quantum synchronization showing that this is a rather resilient phenomenon in these networks.

npj Quantum Information (2018)4:57; doi:10.1038/s41534-018-0108-9

INTRODUCTION

The growing experimental ability in the design, control, and probe of ever larger and increasingly complex coherent quantum systems has recently fueled a newly emerging field combining tools and approaches of complex networks theory with quantum information theory. This cross-disciplinary field aims at understanding static and dynamical properties of complex quantum networks in relation to their topology. Formally, complex quantum networks are distinguished from complex classical networks by the physical nature of the nodes and links composing them.¹ Specifically, complex quantum networks can be grouped into two main classes eventually occurring in the same platform: the first class entails quantum systems whose connections are represented by entangled states,^{2–6} while the second class groups networks wherein the nodes are quantum systems and the links are physical forces or interactions between them.^{7–16} The main application of the first class of complex quantum networks is secure quantum communication,^{7,8,17–19} while the study of networks of the second type is of relevance for understanding quantum transport in both biological and artificial complex systems.^{9,20–27}

One of the key features of complex quantum networks, as opposed to classical ones, is their potential to encode, preserve and exploit crucially quantum properties. Several questions have been raised and investigated in this framework: can we exploit quantum correlations to improve security in network communication?^{7,8,17–19} Does quantum coherence play a role in excitation transfer through networks?^{21,25,26} Can we use a local quantum probe to extract global information on a complex quantum network?^{28–30} Can we use complex quantum networks as quantum simulators of nontrivial open quantum systems?^{28,30,31} How do emergent phenomena known in classical complex networks arise into the quantum regime?^{32–35}

Moving toward scalable multi-component architectures of increasing complexity, it is imperative to understand how resilient are complex quantum networks to the presence of external perturbations. It is well known that quantum-enhanced protocols and devices are extremely sensitive to the presence of noise induced by the surrounding environment,³⁶ though depending on their symmetries quantum systems can display degrees of freedom immune to decoherence.^{13,37–58,59,60}

An extended system, consisting of many components, dissipates into a common bath³⁷ when it is small, so seeing a unique point of the environment.^{38,39} Furthermore, this occurs also for larger systems interacting with different parts across structured environments under some conditions (of components position and frequency).^{44,54,59,60} Collective dissipation and decoherence are known to enable phenomena like superradiance^{38–43} and synchronization,^{32,61,62} allowing for asymptotic entanglement,^{45–48,63,64} and have recently been explored in the context of quantum computation^{37,49–53} metrology,⁵⁵ communications,¹³ and thermodynamics.^{56–58} These phenomena, even when addressed in extended systems, are generally associated with highly symmetric structures, such as pairs of identical components or regular lattices.

Our aim is to assess the resilience of these phenomena and, more in general, of noiseless subspaces in complex networks. We address the existence of noiseless subspaces focusing on the effects of the topology in the paradigmatic example of random Erdős-Rényi quantum networks^{2,12} and also in small-world networks.⁶⁵ We then extend our analysis beyond topology by looking at the resilience for inhomogeneities in parameters. Random quantum networks are shown to support noiseless clusters where quantum coherences can survive indefinitely, allowing one to either store or transport quantum states,

¹IFISC (UIB-CSIC), Instituto de Física Interdisciplinar y Sistemas Complejos, Palma de Mallorca, Spain and ²Turku Centre for Quantum Physics, Department of Physics and Astronomy, University of Turku, FI-20014 Turun yliopisto, Finland

Correspondence: Albert Cabot (albertcabot@ifisc.uib-csic.es) or Roberta Zambrini (roberta@ifisc.uib-csic.es)

Received: 11 June 2018 Accepted: 16 October 2018

Published online: 05 November 2018

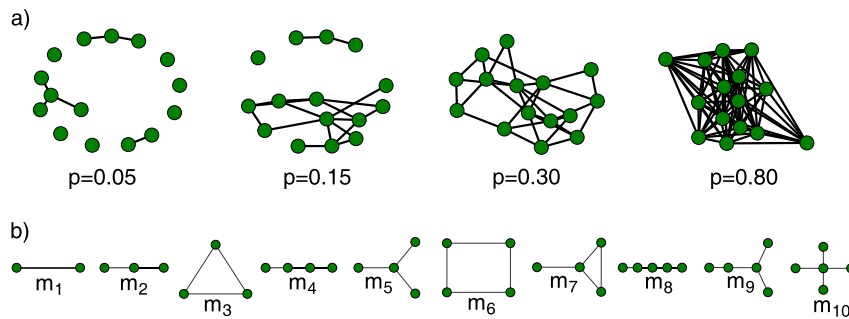


Fig. 1 **a** Realizations of Erdős–Rényi (ER) random networks with 15 nodes, and for different probabilities of connection p . For $p = 0.05$, and $p = 0.10$ the networks are composed by many components, while for $p = 0.30$ and $p = 0.80$ there is only one component spanning all the nodes. **b** Motifs with less than five connections. For small probabilities of connection, the motifs with few connections dominate

excitations or, e.g., entanglement in a virtually error-free way even in the presence of environmental noise. The abundance, the extension and the composition of these decoherence-free substructures are analyzed in different topological regimes. We show (Sect. II.) and discuss (Sect. III.) the presence of a persistent (breathers) feature in the extension of these noiseless structures. We further establish that random quantum networks can embed not only noiseless components, but also a clearly identifiable family of quasi-noiseless ones. We finally address how common is their synchronizability in the transient and asymptotic dynamics. These findings are analyzed and interpreted in connection to the specific characteristics of the complex network topological regimes, discussing their generality, and possible extensions (Sect. III. and Supplementary Information).

RESULTS

We consider a model of interacting quantum harmonic oscillators (nodes) with linear interactions (links), so our system belongs to the second class of complex quantum networks as described above. Reconfigurable and controllable complex quantum networks can be experimentally realized with optical³⁰ as well as circuit QED¹⁶ set-ups, paving the way to new investigations on the interplay between topology and dynamical properties.

Erdős–Rényi quantum networks in a common environment

Erdős–Rényi (ER) random graphs (Fig. 1a) constitute a stochastic mechanism for network generation. Despite being based on minimal assumptions, they exhibit rich phenomenology.^{66,67} Fixing natural N and $0 < p < 1$ as parameter values, the ER statistical ensemble $\mathcal{G}(N, p)$ is over networks with exactly N nodes, assigning probability

$$p^M(1-p)^{N(N-1)/2-M} \quad (1)$$

to a network with M connections. In practice, one draws a network from the ensemble by independently considering each of the $N(N - 1)/2$ unordered node pairs $\{i, j\}$ and establishing the connection between i and j with probability p . For not too small N , this random and uncorrelated creation of connections typically produces a network without obvious symmetries. In the small-world model by Watts and Strogatz,⁶⁵ properties of real networks have been reproduced by an interpolation between the two extremes of random networks and regular lattices.

For the present context, connectedness is a crucial network property. A network is connected if it consists of a single component: for all nodes i and j there is a path or walk from i to j . In ER random graphs, the probability of connectedness $P_{\text{conn}}(N, p)$ increases with p , see Fig. 1a. In fact, the increase of P_{conn} is steepest around $p_c = N^{-1} \ln N$. For large N , the p -dependence of P_{conn} is close to a step function with a value close to zero for $p < p_c$ and close to 1 for $p > p_c$. Here, random networks are introduced to

reveal how the complexity of the connectivity influences the decoherence across medium size networks of N nodes.

Our analysis is valid for physical systems modeled by networks either of harmonic oscillators or coupled spins in presence of a single excitation (Sect. III and Supplementary Information). Here we formally introduce the bosonic Hamiltonian:

$$\hat{\mathcal{H}} = \frac{1}{2} \sum_{i=1}^N (\hat{p}_i^2 + (\omega_i^2 + 2k_m)\hat{q}_i^2) - \sum_{i=1}^N \sum_{j=1}^N \lambda_{ij}(1 - \delta_{ij})\hat{q}_i\hat{q}_j, \quad (2)$$

where \hat{q}_i and \hat{p}_i are position and momentum operators of the quantum harmonic oscillators with frequencies ω_i . The applicability to tight-binding Hamiltonians is discussed in Supplementary Information. Inhomogeneity of frequencies and couplings will be also considered: $\omega_i = \omega_0 + \Delta\omega_i$, $\lambda_{ij} = \lambda_{ji} = \lambda + \Delta\lambda_{ij}$ or (for disconnected nodes) $\lambda_{ij} = \lambda_{ji} = 0$, where $\Delta\omega_i$ ($\Delta\lambda_{ij}$) are zero mean Gaussian numbers with standard deviation $\sigma_\omega(\sigma_\lambda)$. Finally, we have introduced the frequency shift $2k_m$ to ensure that the eigenfrequencies of Hamiltonian (2) are always positive. A sufficient condition adopted here is to set k_m equal to the largest degree of a given network times λ .

Within the formalism of open quantum systems, we consider the complex network dissipating globally into a common bath³⁷ (fully spatially correlated dissipation), leading to cross-damping effects.⁵⁹ Within a microscopic approach, we assume all network nodes (oscillators) identically coupled to a thermal bath. Therefore, the center of mass \hat{q}_{cm} of the network channels collective dissipation. If there are network normal modes perpendicular to \hat{q}_{cm} , these define noiseless clusters. Similarly, for purely dephasing noise and tight-binding Hamiltonian of interest for biological networks,⁶⁸ they define decoherence-free clusters. In order to characterize the details of the full dynamics of the network, for instance to establish the presence of quasi-noiseless clusters or transient synchronization, a master equation (ME) formalism in the weak dissipation limit is considered (sect. IV and refs.^{32,64}). We anticipate that the characterization of noiseless subspaces of the network follows from a symmetry of the total Hamiltonian (i.e., $\hat{\mathcal{H}} + \hat{\mathcal{H}}_B + \hat{\mathcal{H}}_{SB}$ given by Eqs. (2), (3), and (7), respectively), thus its validity is not constrained by approximations introduced when describing the reduced network dynamics with ME (see Sect. IV).

In the following, we study how collective dissipation and the topology of the open network can concur in shielding part of the latter from decoherence. This will enable decoherence-free subspaces (DFSs), noiseless subsystems (NSs) (see for example⁶⁹ and the references therein), or information-preserving structures (IPSSs).⁷⁰ Well-known examples are the simplest cases of two or few qubits^{45–48,71–73} and oscillators.^{63,64,74,75}

Noiseless clusters: abundance and structure

We start our analysis by addressing the simplest case of a network with homogeneous parameters (i.e., $\sigma_\lambda = \sigma_\omega = 0$) and focusing on

the network topology. A convenient property of this model is that the particular values of ω_0 and λ do not influence the shape of the eigenvectors. (This follows from the fact that the constant diagonal elements do not affect the diagonalization of the Hamiltonian, and the remaining λ can be factorized out of the adjacency matrix. Hence our analysis is independent of the couplings strength, and these system parameters only play a role in determining the eigenfrequencies). Our results are therefore determined solely by the topology of the underlying Erdős–Rényi network, which depends only on p and N . Furthermore, the same analysis holds for a tight-binding Hamiltonian with uniform parameters and ER network topology, as the adjacency matrix, in this case, is defined in an equivalent way (Supplementary Information).

Important limit cases are those in which the Hamiltonian matrix is in a shifted Laplacian form (i.e., the sum of every element of any column or row takes the same constant value) as this leads to the center of mass (c.m.) being always an eigenvector of the Hamiltonian (2). Then for shifted Laplacian Hamiltonians, there are always $N - 1$ normal modes perpendicular to the c.m. and thus uncoupled from the bath. Each of these eigenvectors constitutes a NS. It can be easily shown that this is the case for systems described by Hamiltonian (2) with uniform parameters in either fully connected networks or regular lattices. In general, however, the problem of the existence of NSs beyond these highly symmetric configurations is not trivial. This motivates the study of abundance and structure of NSs in random networks for $0 < p < 1$.

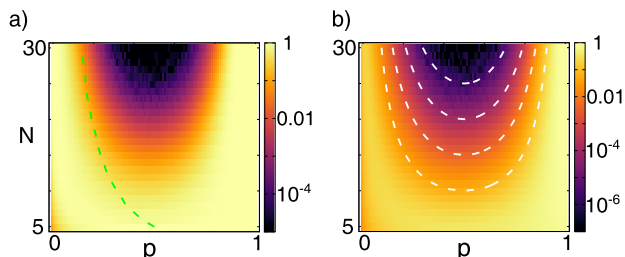


Fig. 2 Probability to find at least one NS (a) and fraction of noiseless normal modes out of the total (b) as a function of the probability of connections in ER network p and its size N . Increasing values appear in lighter color. Green dashed line corresponds to the transition probability above which the probability of connectedness overcomes 50%. White dashed lines are contour plots of the variance of the degree distribution. Parameters are fixed to: $\omega_0 = 2$, $\lambda = 1$. Each point is evaluated over 10^5 realizations

In Fig. 2a, we encode in the color scale the probability to find at least one NS in a network, varying the probability of connection p and the network size N . We remind that in ER networks the average degree is given by the product pN . For small networks there is a significant probability to find a NS for all the range of p 's (bright regions), however, as we increase the size of the networks this region shrinks and it remains significant only at the extreme values of p . The case of $p = 1$ corresponds to the fully connected network limit anticipated above (with $N-1$ noiseless eigenvectors), while for independent oscillators ($p = 0$) the system is fully degenerate and can be always initialized to evolve in a NS. These features are robust when looking at the total fraction of NSs with respect to the N degrees of freedom and we find similar results in Fig. 2b. An interesting issue is about the relation between the underlying topology and the abundance of noiseless normal modes. The green dashed line in Fig. 2a indicates the transition probability to a one large component. In particular, we numerically determine a threshold \tilde{p}_c as the value of p for which $P_{\text{conn}}(N, p) = 1/2$. For networks of $N = 15$ nodes, we observe $\tilde{p}_c \approx 0.23$ (Supplementary Information). White dashed lines in Fig. 2b represent contour plots of the variance of the degree distribution, with inner lines corresponding to higher values. Both quantities give insight on the relevant topological features to have NSs as discussed in detail in Sect. III. In particular, the green line separates the parameter region in which NSs are made of disconnected motifs, from the one in which they are embedded in a large component. The white contours are an indicator of topological disorder (the bigger the variance the less degree homogeneity) which seems to be the key detrimental feature for the abundance of NSs.

For the NSs that are not degenerate, we can characterize their features starting from their extension, i.e., their number of nodes within the network. Thus we introduce the noiseless subsystem size (NS size) as the number of oscillators spanned by a given noiseless eigenvector. Due to the non-degeneracy and with each component's submatrix diagonalizable separately, each NS spans oscillators inside only one connected component. The distribution of sizes of connected components is an important characteristic of ER random networks with fixed p as it indicates different topological regimes (Fig. 1a). In Fig. 3, we represent the probability to find a NS of a particular size (vertical axis) embedded in a network component of a given size (horizontal axis) below the connectedness transition ($p = 0.05$ (a)) and for a connected network ($p = 0.80$ (b)).

For small p , NSs with few nodes predominate as expected, Fig. 3a, while for $p = 0.80$ there is only one component spanning all the oscillators, Fig. 3b. What is surprising is the abundance of NSs spanning over an even number of oscillators (e.g., 2, 4, 6 in Fig. 3a) with respect to the scarce ones that span over an odd number of

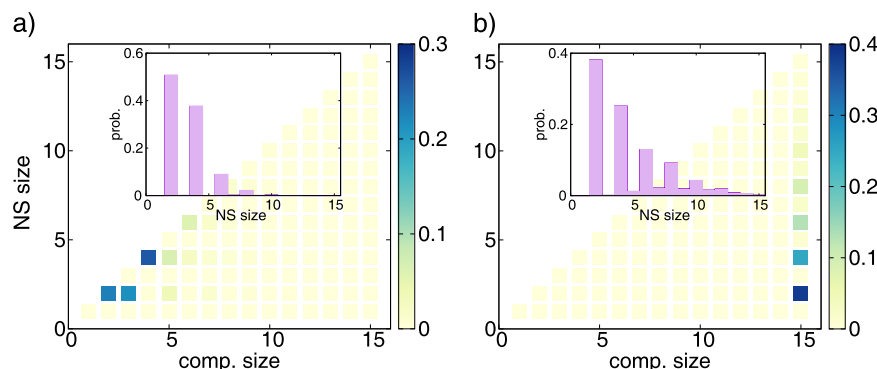


Fig. 3 In color: probability that a NS of a given size (vertical axis) is located in a component of a particular size (horizontal axis), with $N = 15$, and $p = 0.05$ (a) or $p = 0.80$ (b). Both in a and b, we have not taken into account degenerate subspaces. Both insets show the distribution of sizes of NSs, obtained by summing all the contributions from different component sizes to the same NS size

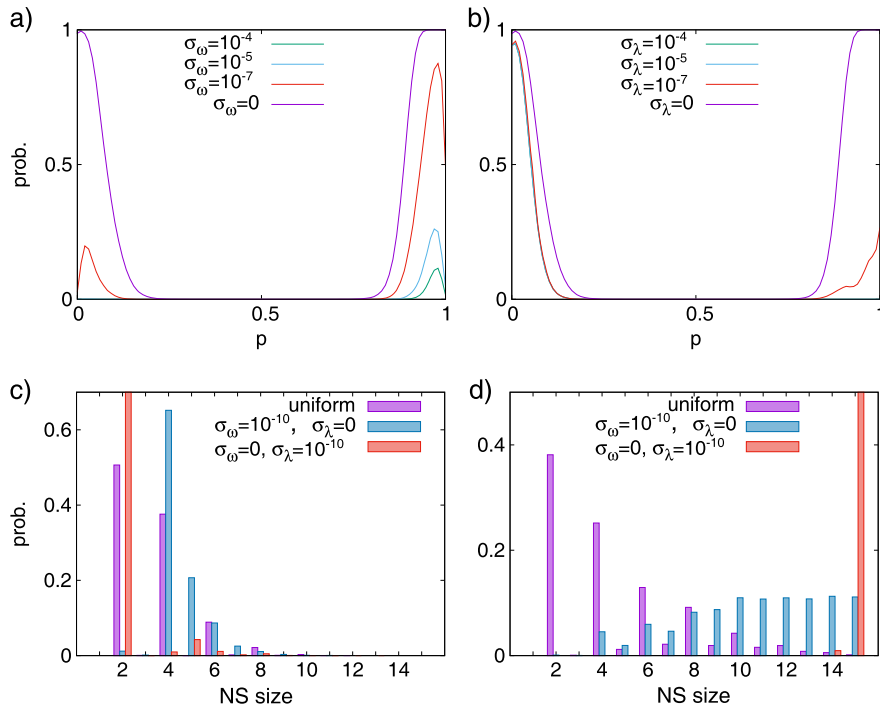


Fig. 4 **a, b** Probability to find at least one decoherence-free normal mode for $N = 30$, for inhomogeneous frequencies with different σ_ω values (a), for inhomogeneous couplings with different σ_λ (b). **c, d** Probability distribution of NSs of different sizes (i.e., number of nodes of the noiseless eigenvector) for nonuniform frequencies (in blue, for $\sigma_\omega = 10^{-10}$) and couplings (in red, for $\sigma_\lambda = 10^{-10}$), in purple uniform parameters. Parameters $N = 15$ and $p = 0.05 < \bar{p}_c$ (c), $p = 0.80 > \bar{p}_c$ (d)

oscillators. This happens independently from the parity of the size of connected components (look for instance at components of sizes 4 and 5 in Fig. 3a) and of N (not shown). In the case of components of odd size (for example of size 5), this implies that at least one of the oscillators is not involved in its largest NS (with 4 nodes in this example). Interestingly, this characteristic parity symmetry in the NS size distribution is rather robust, and also observed for large probabilities of connection, as in (b) and also in small-world networks (Supplementary Information). The origin of this parity feature of NSs will be shown to be related to the presence of breathing modes and discussed in Sect. III.

Resilience in presence of imperfections

The study of homogeneous networks—with identical local frequencies and coupling strengths—allows to isolate the importance of the topological features for the existence of NSs. Here, we consider their resilience in the presence of not uniform parameters, as they would occur for instance in biological complexes or any experimental set-up, inevitably characterized by inhomogeneity and imperfections. We consider Gaussian distributions either in frequencies or couplings ($\sigma_{\omega,\lambda} \neq 0$). Very small inhomogeneities ($\sigma_{\omega,\lambda} \sim 10^{-10}$) are enough to remove degeneracy in normal modes, while the probability to find NSs does not significantly change. In Fig. 4a, b, we show the results of increasing differences on frequencies (a) and couplings (b) for the probability to find at least one NS. NSs can be very fragile even for small deviations from the uniform parameters. Important exceptions occur for inhomogeneous couplings that do not affect NSs for small components (Fig. 4b for $p \lesssim 0.2$). Otherwise, large components are more resilient to the presence of detunings across the network, Fig. 4a.

Also, the structure of NSs is strongly influenced by inhomogeneous parameters (Fig. 4). Looking at the regime where small components dominate (for $p = 0.05$, Fig. 4c), detuning (blue) leads to the disappearance of NSs of just pairs of nodes, as expected;

decoherence-free normal modes spanning over four oscillators are the most common (even if embedded in motives of five oscillators, not shown). In the regime of one large component (for $p = 0.8$, Fig. 4d), NSs can have different sizes spanning from four oscillators to the whole network. In both cases, detuning removes the even–odd asymmetry. In networks with nonuniform coupling strengths (red histograms in Fig. 4), NSs of two oscillators survive and predominate for small p (c), while for high p the decoherence-free mode is extended over almost all the network (d).

Quasi-noiseless clusters

We have seen that in general inhomogeneity in the parameters across the network is detrimental for NSs. On the other hand, for practical purposes, it can be more interesting to establish if there are some modes with very long (even if not infinite) decoherence times. In this spirit, we ask whether in spite of inhomogeneity there is still a well-defined set of modes which, although not perfectly decoupled from the bath, dissipate more weakly than the rest, being effectively frozen over long time scales.^{32,64}

We introduce then quasi-noiseless clusters that can be identified looking at their overlap, named κ , with the lossy mode \hat{q}_{cm} (see Sect. IV). Figure 5 represents the probability to have quasi-noiseless modes depending on detuning (σ_ω on the vertical axis) and on their overlap κ (horizontal axis). Then decoherence-free modes do correspond to the first column ($\kappa \leq 10^{-13}$, our numerical zero), and the uniform ER network case to the lowest row. We observe that uniform networks exhibit two very well-defined sets of normal modes (left and right in Fig. 5), separated by a huge gap in their respective dissipation rates (as quantified by κ): this gap allows to properly distinguish (and characterize even numerically) NSs with respect to the others.

As we increase the spread in detunings σ_ω , NSs tend to become slightly more noisy, with predominance of modes for $\kappa \sim \sigma_\omega$ (diagonal in Fig. 5). The gap between quasi-noiseless and

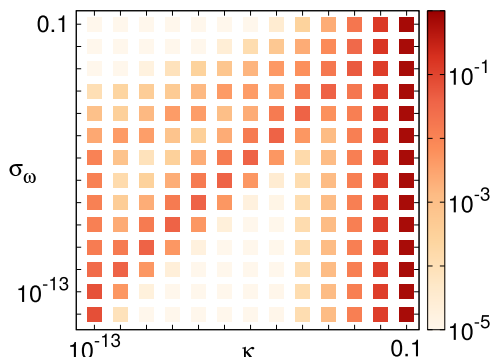


Fig. 5 Probability to find a normal mode with a certain overlap with the dissipative mode (κ) and in presence of detuning across the network with variance σ_ω . The values for κ are binned according to their order of magnitude, i.e., the column 0.01 corresponds to normal modes with κ of the order of 0.01. The results have been obtained for networks of size $N=30$ and $p=0.9$.

dissipating normal modes decreases. Despite strict decoherence-free modes tend to disappear for increasing inhomogeneity, two well separate sets of normal modes (with a significant gap in κ) survive up to a certain strength σ_ω . This allows to identify quasi NSs up to a certain degree of disorder in frequencies. Analogous results are found for nonuniform couplings, i.e., for non-zero σ_λ .

Synchronization

In this section, we focus on the emergence of synchronous dynamics induced by collective dissipation.⁶¹ Several coupled qubits or harmonic oscillators can exhibit persistent and synchronous oscillations in presence of dissipation in a common environment, as different dissipation rates are induced in the system normal modes. This synchronization mechanism was already described in refs. ^{32,33,74}, after a transient in which each node oscillates irregularly in a superposition of eigenfrequencies, all normal modes, except the one with the slowest decay, relax to equilibrium. Then, this slowest mode fixes the common rhythm of the corresponding nodes within the network either during a long transient or—when the slowest mode is actually noiseless—asymptotically. Synchronization can be identified also in quantum systems comparing the dynamics of local observables (for a review of different approaches see ref. ⁶¹). In particular, dissipation-induced synchronization has been addressed for arrays of oscillators,^{32,33,74,76} spins,^{34,62,77} self-sustained oscillations in optomechanical systems,⁷⁸ and also reported for random topology in harmonic networks.³² Nevertheless, the role of the network structure has not been addressed before.

For this analysis, we assume that the oscillators follow the Born–Markov master Eq. (8). Building on previous works, we can focus on the normal modes decay rates to determine the emergence of mutual synchronization in the oscillators array.⁶¹ We recall the conditions for which a motif of any network of harmonic oscillators synchronizes as reported in refs. ^{32,33,74}: (i) when one of the normal modes covering the particular subset of oscillators is coupled more weakly to the bath than the others (significant separation of dissipative time scales), leading to *transient synchronization*,³³ or (ii) when there is only one decoherence-free normal mode covering the particular subset of oscillators, leading to *stationary synchronization*.^{32,74} In case (i) we set as a significant separation of dissipative time scales when the smallest and second smallest dissipation rates are separated by an order of magnitude,³² i.e., their ratio, R , takes values at most of order $R \sim 0.1$ (see section IV. for definitions). When this condition is satisfied, after most normal modes dissipate out, there remains only the slowest one, i.e., the one with the smallest coupling to the

bath, and the oscillators spanned by this normal mode synchronize and can retain robust quantum correlations.^{32,33,74} If R is small there is a significant time period in which the network is synchronous before full thermalization. Conditions (i) and (ii) refer to a particular subset of the network, and of course in the whole network there might be parts of it in which there is synchronization due to mechanism (i) and parts of it in which it is due to (ii), since both mechanisms are not excluding as long as the synchronizing normal modes span over different subsets of oscillators or oscillate at the same frequency.

In Fig. 6, we analyze dissipative synchronization for ER networks, both with uniform parameters and with detuning $\sigma_\omega \neq 0$. The appearance of stationary synchronization shown in Fig. 6a (green line) behaves similarly to the abundance of NSs (see Fig. 4) except for p close to 1 where a dip appears. On the other hand, transient synchronization (Fig. 6a, purple line) is a rather robust feature of the network, present with a significant probability (about in one over three networks) in all the range of p 's except for a dip appearing again at p close to 1, where stationary synchronization dominates. In panel (b), we look at the effect of detuning, both for a specific average degree (for $p=0.5$) and on average overall values of p . Transient synchronization is found to be rather resilient to detuning (purple line) while stationary synchronization (ii) is more fragile, as expected knowing results about NSs resilience reported in previous sections. Analogous results are found for nonuniform couplings.

What about the structure of the synchronous modes? Decoherence-free synchronized normal modes (ii) tend to span a small number of oscillators and the even–odd asymmetry reported before persists (Fig. 6c, green histogram). More surprising is the fact that transient synchronization (i), beyond being a rather frequent phenomenon for several p and detunings, it does also tend to span all the network (Fig. 6c, purple), which means that a large set of oscillators synchronize and will, therefore, as previously reported in refs. ^{32,33}, share enhanced quantum correlations. The time scale to observe this phenomenon can be assessed through the decays ratio R : the fastest rise of synchronization corresponds to smallest R values.³² A significant synchronous transient is predicted before thermalization: in Fig. 6d, the distribution of ratios R for $\sigma_\omega = 0$ shows, in fact, significant fractions of networks with more than two orders of magnitude of separation between the slowest decaying modes. This is weakly influenced by the network structure and displayed aggregating data for different p values.

DISCUSSION

Insight about our results on the abundance and structure of NSs (Figs. 2 and 3) can be gained, considering the underlying network topology and regimes, dominated by small and large size components (small and larger p 's in Fig. 3). Above a certain value of p , networks are composed predominantly by a single component (see Supplementary Information for distributions of component sizes for different p 's). The corresponding disappearance of small components is what crucially hinders the existence of noiseless modes for small p as clear by the comparison in Fig. 2a: below the threshold probability \bar{p}_c (green dashed line), several small components exist. Furthermore, the most abundant linear motifs (such as m_1, m_2, m_4, \dots) in ER networks, Fig. 1b represent in this case noiseless modes,⁷⁴ determining the abundance of NSs.

What about networks with larger average degree? The degree distribution of Erdős–Rényi networks is known to be binomial, with variance $(N-1)p(1-p)$. A spread of the degree distribution is a good measure of the inhomogeneity of the network topology being maximal at $p=0.5$ (with maximum value increasing with the size of the network N) and minimal at 0 and 1 (see also SI). The comparison of this variance with the NSs abundance in Fig. 2b (with inner contours corresponding to larger values of this

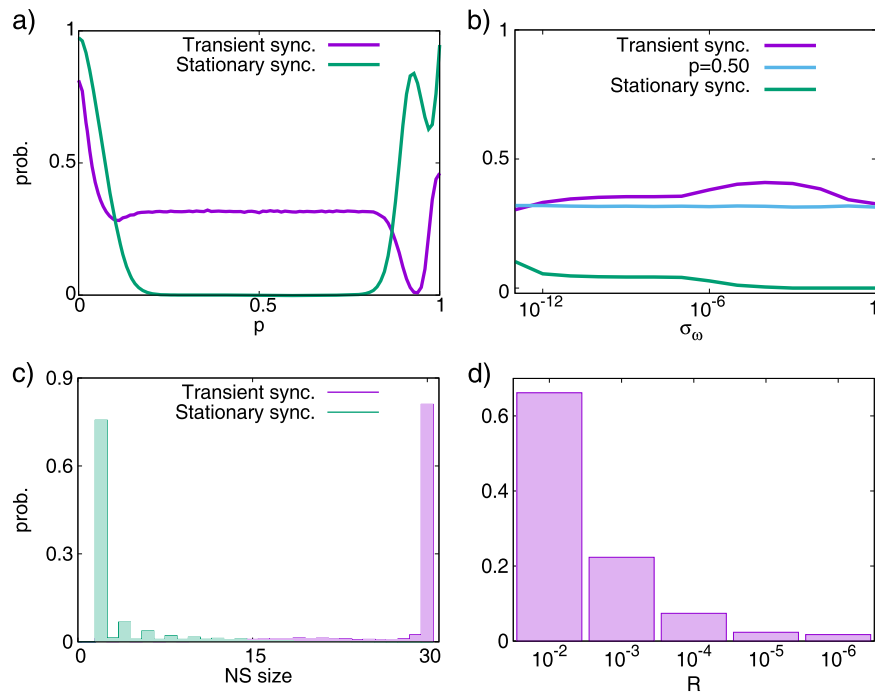


Fig. 6 For all the panels, we consider ER networks of size $N=30$. **a** Probability to find at least one synchronized normal mode which is stationary (green) or transient (purple), varying p , and with uniform parameters. **b** Probability to find at least one synchronized normal mode per network as a function of the detunings spread σ_ω : for transient synchronization when $p=0.5$ (blue) and when averaging overall p 's (purple) and for stationary synchronization when averaging overall p 's (green). **c** Distribution of sizes for the case of stationary and transient synchronized normal modes, for $\sigma_\omega=0$ and all the range of p 's, and again for $\sigma_\omega=0$. **d** Distribution of values of R for dissipating normal modes (avoiding completely NSs) for all the range of p 's, and again for $\sigma_\omega=0$.

variance) allows to establish a clear quantitative connection. The network topological uniformity is indeed found to be a crucial ingredient for the abundance of noiseless modes also when looking at other networks. Small-world networks, for instance, also display a transition to disorder starting from a regular lattice with a certain degree and randomly rewiring the nodes until becoming a random network (Supplementary Information). Also in this case, as disorder in the topology increases, noiseless mode abundance diminishes, indicating a robust relation between homogeneity in network topology and presence of NSs. A further measure that could be explored would be a distance between the actual Hamiltonian of the system and the “nearest” Hamiltonian in shifted Laplacian form, for which we have pointed out that NSs are predicted.

A main and intriguing feature of NSs in uniform ER networks is the parity of their sizes, that is the fact that decoherence-free normal modes tend to be composed by an even number of oscillators, Fig. 3a, b. The absence of NSs with odd sizes, independently on the odd or even size of the embedding component, can be traced back to the fact that for small values of p string-like components of the network prevail, like motifs $m_{1,2,4,8}$ in Fig. 1b. In these kinds of motifs, we can actually identify stretching or breathing normal modes which are decoherence-free and which involve all the string for an even motif, while they do not involve the central node for an odd motif, as discussed in the case of three oscillators in ref. ⁷⁴. The presence of these breathing modes of even size allows to explain the predominance of even NSs below the connectedness transition. Above the connectedness transition, Fig. 3b, we can show (Supplementary Information) that by embedding the small motifs of Fig. 1b (and also those of Fig. S5 of the SI) into the network with the proper symmetries in the connections, the noiseless eigenvectors of these motifs become noiseless eigenvectors of the whole system. This allows us to clarify why we observe a similar structure in the NSs size when considering very connected ER networks (Fig. 3b), where

homogeneity in the degree distribution can enable the necessary symmetries in the couplings to be satisfied frequently. It is important to stress that we find this peculiar even modes dominance also for small-world networks (SI), which are composed mainly by one component, and which tend to display bigger noiseless modes than ER networks. As a further remark, detuning is known to introduce deviation from breathing modes,⁷⁴ and this is consistent with the absence of even–odd asymmetry for NSs shown in Fig. 4d. These decoherence-free breathing modes also dictate the form of stationary synchronization as shown in Fig. 6c. Finally, there is a noteworthy resemblance between the small NSs observed here, and the compact localized states that can be found in certain tight-binding lattices.⁷⁹ Also these localized states are often perpendicular to the c.m., and the enabling mechanism is the proper local topology of connections between the involved nodes and the neighboring lattice (see illustrative examples in refs. ^{80–82}). The exploration of the connections between these two different contexts could constitute an interesting future extension to our work.

Beyond topological features, we have considered inhomogeneous parameters for nodes and links as these can actually be unavoidable in experiments.^{16,30} For the frequency combs platform,³⁰ this experimental analysis has not yet been reported but the possibility to achieve identical nodes is discussed in ref. ⁸³ through chirping of the pump optical mode. On the other hand, a small amount of disorder has been measured in circuit QED lattices⁸⁴ and modeled as Gaussian as in our analysis. Frequency disorder up to $\sigma_\omega \sim 10^{-4}$ has been reported, that would significantly hinder NSs (Fig. 4), while inhomogeneities in (small) coupling rates are mainly induced by detunings and can be neglected in circuit QED networks.⁸⁴ We have analyzed both frequency and couplings disorder: for small connection probabilities, NSs are fragile against detuning but not against inhomogeneities in couplings, and the opposite trend is found for large components (Fig. 4). This can be understood to follow from the

fact that small decoherence-free normal modes are more sensitive to inhomogeneity in frequencies. Motifs of two oscillators, for instance, are NSs independently of the value of the coupling and only if their frequencies are identical,³³ while NSs for m_2 motifs appear only for special values of detunings,⁷⁴ consistently with the NSs resilience found for small p 's. For both detuning and couplings inhomogeneities, Fig. 4, the drop in the probability at $p = 1$ follows from the fact that the corresponding fully connected network, in the case of Gaussian distributed parameters, has no NSs. The presence of even small inhomogeneities allows also to avoid degenerate eigenvectors particularly abundant for $p \sim 0$ and $p \sim 1$.

Despite the fragility of NSs to inhomogeneities in parameters observed in Fig. 4, we have seen in Fig. 5 the existence of quasi-noiseless components up to moderate values of disorder ($\sigma_\omega > 0$). The gap in the coupling with the environment of two sets of normal modes allows to clearly identify quasi-noiseless subspaces dissipating much slower than other modes. The closure of the gap for $\kappa \sim \sigma_\omega$ can be understood considering that in the limit of small detuning, normal modes will deviate linearly in σ_ω from the NSs found for uniform ER networks. These quasi-NSs that persist in inhomogeneous networks can be useful for practical applications: even if manufacturing imperfections would prevent the existence of asymptotically decoherence-free modes, the long coherence time of quasi NSs can serve the purpose of preserving coherences on time scales proportional to the degree of inhomogeneity of the device.

Finally, we discuss in more detail some of the features observed in the study of synchronization. We have seen that the probability of transient synchronization is large and resilient in presence of inhomogeneous detunings. Surprisingly, it can even be favored by increasing detuning (as shown in Fig. 6b, purple line), and this might be caused by the corresponding disappearance of stationary synchronization. The fact that this increase is seen when looking at the aggregated data in p , while for $p = 0.5$ (blue line) is not observed, is consistent with our explanation, as for $p = 0.5$ there are no NSs independently of σ_ω . We have also observed that there is a dip in the probability to find synchronization for p close to 1 (Fig. 6a). These dips appearing for high p both for stationary and transient synchronization are related to the increasing probability to find large NSs of modes in the same network, of different frequencies, diminishing the overall synchronizability of networks. As p is further increased, degeneracy also grows and overlap between synchronizable modes is no longer detrimental as they exhibit the same frequency, hence explaining the final increase in the synchronization probability.

It is important to assess the generality of our findings in other random networks. We first notice that we have considered a dipole-dipole coupling in Hamiltonian (2). One can wonder if similar results would hold if we consider instead systems with spring-like coupling Hamiltonian $\hat{\mathcal{H}} = \frac{1}{2} \sum_{i=1}^N (\hat{p}_i^2 + \omega_0^2 \hat{q}_i^2) + \sum_{i=1}^N \sum_{j=1}^N \lambda_{ij} (\hat{q}_i - \hat{q}_j)^2$, where all the oscillators have the same frequency, and the coupling λ_{ij} can take the values λ or zero. It can be shown (Supplementary Information) that in this case there are always $N - 1$ NSs whatever is the underlying topology. We can also consider a tight-binding model, and in this case, our results would still hold in the case of networks with homogeneous parameters (Supplementary Information). Finally, in presence of a single excitation, our analysis would also apply to spin or fermionic networks while the case of more excitations is an open question.

An essential aspect of the model used is the equal coupling of the nodes to the common bath, relevant in the contexts of densely packed pigment-protein complexes,^{85–87} and superradiance experiments.^{40–43} In particular, in the context of quantum transport through biological structures, experimental evidence for strong spatial correlations in bacterial reaction center dynamics⁸⁵ and conjugated polymers⁸⁶ has been obtained, and correlated

noise has also been predicted to be relevant in other photosynthetic complexes.⁸⁷ These structures are rather large and complex in their topology, presenting also non-homogeneous site energies and couplings. It is to be noted that excitation transfer in biological complexes might be governed by a dephasing model that can present decoherence-free (instead of dissipation-free) clusters.

Further possible extensions of this work could establish the effects of relaxing the constant coupling to the bath through the network: in this case another noisy channel—instead of the center of mass—arises and new features are expected. The bath can also be considered as an extended system,^{59,60} hence the nodes of the network system will interact with different parts of the environment. This structured environment would give rise to a rich scenario of correlated dissipations for the network. Other forms of collective dissipation can be further explored to model bulk systems dissipating mainly through their surface.⁸⁸ Finally, our analysis of NSs in networks is valid also in the non-Markovian dissipation regime, as it relies on a symmetry of the full system-environment Hamiltonian, while non-Markovian effects due to strong coupling with the environment could be explored in the context of quasi-noiseless modes and transient synchronization.

The possibility to shield complex networks nodes by decoherence, not only in symmetric lattices, but in complex networks, opens the way to studies of storage or transport of quantum states, excitations or entanglement in structures with increasing complexity. The impact of different topologies can be explored in the mentioned contexts of quantum computation^{37,49–53} metrology,⁵⁵ communications,¹³ and thermodynamics,⁸⁹ and explored for other forms of correlated dissipation. It could also help understanding why nature has chosen some network structures as ultra-optimized transport architectures for energy harvesting,⁸⁹ and to identify strategies for quantum computing based on NSs. These predictions can be tested in different timely platforms, both photonic³⁰ and in circuit QED.¹⁶

METHODS

In this section, we write down the Hamiltonian model describing the thermal bath and the interaction with the system. Later on, we derive the condition for a normal mode to be uncoupled from the bath and we show how this leads to dissipation-free dynamics. The results presented in this section have been derived in detail in ref. ³².

The thermal bath is composed by an infinite collection of harmonic oscillators at thermal equilibrium:

$$\hat{\mathcal{H}}_B = \frac{1}{2} \sum_{a=1}^{\infty} \left(\frac{\hat{K}_a^2}{M_a} + \nu_a^2 \hat{X}_a^2 \right), \quad (3)$$

where the position and momentum operators of the bath modes follow the canonical commutation relations $[\hat{X}_a, \hat{K}_\beta] = i\hbar \delta_{ab}$. The system-bath interaction is described by:

$$\hat{\mathcal{H}}_{SB} = -\sqrt{\gamma} \sum_{n=1}^N \hat{q}_n \hat{B}, \quad \hat{B} = \sum_a \lambda_a \hat{X}_a, \quad (4)$$

from which, we can appreciate that the system interacts with the environment through the c.m. coordinate, $\hat{q}_{cm} = \sum_{n=1}^N \hat{q}_n$. It is insightful to write the system-bath Hamiltonian in terms of the normal modes of the system defined as:

$$q = \mathcal{F}Q, Q = \mathcal{F}^T q, \Rightarrow \hat{q}_n = \sum_{m=1}^N \mathcal{F}_{nm} \hat{Q}_m, \hat{Q}_n = \sum_{m=1}^N \mathcal{F}_{mn} \hat{q}_m, \forall n \quad (5)$$

where $Q = (\hat{Q}_1, \dots, \hat{Q}_N)^T$, $q = (\hat{q}_1, \dots, \hat{q}_N)^T$ and \mathcal{F} is the rotation diagonalizing the system Hamiltonian (2), i.e.:

$$\hat{\mathcal{H}} = p^T \frac{1}{2} p + q^T \mathcal{M} q = P^T \frac{1}{2} P + Q^T \mathcal{D} Q = \frac{1}{2} \sum_{n=1}^N (\hat{p}_n^2 + \Omega_n^2 \hat{Q}_n^2), \quad (6)$$

where 1 is the identity matrix, \mathcal{M} is the matrix containing the frequencies and couplings as prescribed in (2), and $\mathcal{D} = \mathcal{F}^T \mathcal{M} \mathcal{F}$ is the diagonal matrix containing the system eigenfrequencies Ω_n . In the normal mode basis, the

system bath Hamiltonian reads as:

$$\hat{\mathcal{H}}_{SB} = -\sqrt{\gamma} \sum_{n=1}^N \kappa_n \hat{Q}_n \hat{B}, \quad \kappa_n = \sum_{m=1}^N \mathcal{F}_{mn}, \quad (7)$$

hence each normal mode is coupled to the bath with its own rate that depends on the matrix diagonalizing the system (and thus on the topology and parameters of the system). Importantly, if $\kappa_n = 0$ the mode n is uncoupled from the bath, which can be stated equivalently as the normal mode n being perpendicular to the c.m. (recall that $\hat{Q}_n = \sum_{m=1}^N \mathcal{F}_{mn} \hat{q}_m$, i.e., the scalar product with \hat{q}_{cm} is proportional to κ_n).^{32,74}

In the normal mode basis, the full Hamiltonian describing the system, the bath, and their interaction, is given by adding terms (3), (6), and (7). From this total Hamiltonian, we readily see that an immediate consequence of $\kappa_n = 0$ is that degrees of freedom of the mode n , i.e., Q_n and \hat{P}_n , commute with the system–bath interaction term (7). Therefore, the reduced dynamics of this mode is not influenced by dissipation, indeed it is unitary and described just by $\frac{1}{2}(\hat{P}_n^2 + \Omega_n^2 \hat{Q}_n^2)$. Hence the *noiseless condition* stems out of a symmetry of the total Hamiltonian, and is independent of the subsequent approach used to approximate the dynamics of those normal modes which are coupled to the thermal bath.

The analysis of transient synchronization in the network follows ref. ³², and is valid in the weak system–bath coupling limit under standard Born–Markov approximations leading to the Lindblad master equation ($\hbar = 1$):

$$\begin{aligned} \frac{d\hat{\rho}(t)}{dt} = & -i[\hat{\mathcal{H}}, \hat{\rho}(t)] \\ & - \frac{i}{4} \sum_{n=1}^N \Gamma_n ([\hat{Q}_n, \{\hat{P}_n, \hat{\rho}(t)\}] - [\hat{P}_n, \{\hat{Q}_n, \hat{\rho}(t)\}]) \\ & - \frac{1}{4} \sum_{n=1}^N D_n \left([\hat{Q}_n, [\hat{Q}_n, \hat{\rho}(t)]] - \frac{1}{\Omega_n^2} [\hat{P}_n, [\hat{P}_n, \hat{\rho}(t)]] \right), \end{aligned} \quad (8)$$

with $\Gamma_n = \kappa_n^2 \gamma$, and $D_n = \kappa_n^2 \gamma \Omega_n \coth(\Omega_n/2k_B T)$. In order to establish the emergence of dissipation-induced synchronization, one can compare the damping rates of the network normal modes focusing on the ratio R between the two slowest (non-vanishing) rates.³²

DATA AVAILABILITY

This is a theoretical paper and there is no experimental data available beyond the numerical simulation data described in the paper.

ACKNOWLEDGEMENTS

The authors acknowledge support from the Horizon 2020 EU collaborative project QuProCS (Grant Agreement No. 641277), MINECO/AEI/FEDER through projects NoMaQ FIS2014-60343-P, EPheQuCS FIS2016-78010-P, SPASIMM FIS2016-80067-P, and the María de Maeztu Program for Units of Excellence in R&D (MDM-2017-0711). A.C. acknowledges funding from CAIB PhD program and SURF@IFISC internship program. K.K. acknowledges funding from Ministerio de Economía, Industria y Competitividad through the Ramón y Cajal program. S.M. acknowledges the UIB program of invited professors, the Academy of Finland Centre of Excellence program (Project no. 312058) and the Academy of Finland (Project no. 287750).

AUTHOR CONTRIBUTIONS

R.Z., F.G., V.M.E. designed the project, A.C. performed the analysis. All authors contributed to the discussion of results with complementary quantum (A.C., F.G., S.M., R.Z.) and classical (K.K., V.M.E.) perspectives. All authors participated in the writing of the paper.

ADDITIONAL INFORMATION

Supplementary Information accompanies the paper on the *npj Quantum Information* website (<https://doi.org/10.1038/s41534-018-0108-9>).

Competing interests: The authors declare no competing interests.

Publisher's note: Springer Nature remains neutral with regard to jurisdictional claims in published maps and institutional affiliations.

REFERENCES

- Biamonte, J., Faccin, M. & De Domenico, M. Complex networks: from classical to quantum, Preprint at arXiv:1702.08459 (2017).
- Perseguers, S., Lewenstein, M., Acín, A. & Cirac, J. I. Quantum random networks. *Nat. Phys.* **6**, 539–543 (2010).
- Acín, A., Cirac, J. I. & Lewenstein, M. Entanglement percolation in quantum networks. *Nat. Phys.* **3**, 256–259 (2007).
- Perseguers, S., Lapeyre, G. J., Cavalcanti, D., Lewenstein, M. & Acín, A. Distribution of entanglement in large-scale quantum networks. *Rep. Prog. Phys.* **76**, 096001 (2013).
- Cuquet, M. & Calsamiglia, J. Entanglement percolation in quantum complex networks. *Phys. Rev. Lett.* **103**, 240503 (2009).
- Roslund, J., Medeiros de Araujo, R., Jiang, S., Fabre, C. & Treps, N. Wavelength-multiplexed quantum networks with ultrafast frequency combs. *Nat. Photonics* **8**, 109–112 (2014).
- Kimble, H. J. The quantum internet. *Nature* **453**, 1023–1030 (2008).
- Komar, P. et al. A quantum network of clocks. *Nat. Phys.* **10**, 582–587 (2014).
- Ritter, S. et al. An elementary quantum network of single atoms in optical cavities. *Nature* **484**, 195–200 (2012).
- Lodhal, L. Quantum-dot based photonic quantum networks, Preprint at arXiv:1707.02094 (2017).
- Goldstein, S. et al. Decoherence and interferometric sensitivity of boson sampling in superconducting resonator networks. *Phys. Rev. B* **95**, 020502(R) (2017).
- Wiersma, D. S. Random quantum networks. *Science* **327**, 1333–1334 (2010).
- Reiserer, A. et al. Robust quantum-network memory using decoherence-protected subspaces of nuclear spins. *Phys. Rev. X* **6**, 021040 (2016).
- Krenn, M., Gu, X. & Zeilinger, A. Quantum experiments and graphs: multiparty states as coherent superpositions of perfect matchings. *Phys. Rev. Lett.* **119**, 240403 (2017).
- Xuereb, A., Genes, C., Pupillo, G., Paternostro, M. & Dantan, A. Reconfigurable long-range phonon dynamics in optomechanical arrays. *Phys. Rev. Lett.* **112**, 133604 (2014).
- Kollar, A. J., Fitzpatrick, M., Houck, A. A. Hyperbolic lattices in circuit quantum electrodynamics, Preprint at arXiv:1802.09549 (2018).
- Diamanti, E., Lo, H.-K., Qi, B. & Yuan, Z. Practical challenges in quantum key distribution. *NPJ Quantum Inf.* **2**, 16025 (2016).
- Cirac, J. I., Zoller, P., Kimble, H. J. & Mabuchi, H. Quantum state transfer and entanglement distribution among distant nodes in a quantum network. *Phys. Rev. Lett.* **78**, 3221 (1997).
- Paparo, G. D. & Martin-Delgado, M. A. Google in a quantum network. *Sci. Rep.* **2**, 444 (2012).
- Faccin, M., Migda, P., Johnson, T. H., Bergholm, V. & Biamonte, J. D. Community detection in quantum complex networks. *Phys. Rev. X* **4**, 041012 (2014).
- Olaya-Castro, A., Lee, C. F., Olsen, F. F. & Johnson, N. F. Efficiency of energy transfer in a light-harvesting system under quantum coherence. *Phys. Rev. B* **78**, 085115 (2008).
- Galiceanu, M. & Strunz, W. T. Continuous-time quantum walks on multilayer dendrimer networks. *Phys. Rev. E* **94**, 022307 (2016).
- Tsomokos, D. I. Quantum walks on complex networks with connection instabilities and community structure. *Phys. Rev. A* **83**, 052315 (2011).
- Mulken, O., Dolgushev, M. & Galiceanu, M. Complex quantum networks: from universal breakdown to optimal transport. *Phys. Rev. E* **93**, 022304 (2016).
- Campos Venuti, L. & Zanardi, P. Excitation transfer through open quantum networks: three basic mechanisms. *Phys. Rev. B* **84**, 134206 (2011).
- Huelga, S. F. & Plenio, M. B. Vibrations, quanta and biology. *Contemp. Phys.* **54**, 181–207 (2013).
- Chin, A. W., Datta, A., Caruso, F., Huelga, S. F. & Plenio, M. B. Noise-assisted energy transfer in quantum networks and light-harvesting complexes. *New J. Phys.* **12**, 065002 (2010).
- Nokkala, J., Galve, F., Zambrini, R., Maniscalco, S. & Piilo, J. Complex quantum networks as structured environments: engineering and probing. *Sci. Rep.* **6**, 26861 (2016).
- Nokkala, J., Maniscalco, S. & Piilo, J. Local probe for connectivity and coupling strength in quantum complex networks. *Sci. Reps.* **8**, 13010 (2018).
- Nokkala, J. et al. Reconfigurable optical implementation of quantum complex networks. *New J. Phys.* **20**, 053024 (2018).
- Vasile, R., Galve, F. & Zambrini, R. Spectral origin of non-Markovian open-system dynamics: A finite harmonic model without approximations. *Phys. Rev. A* **89**, 022109 (2014).
- Manzano, G., Galve, F., Giorgi, G. L., Hernandez-Garcia, E. & Zambrini, R. Synchronization, quantum correlations and entanglement in oscillator networks. *Sci. Reps.* **3**, 1439 (2013).
- Giorgi, G. L., Galve, F., Manzano, G., Colet, P. & Zambrini, R. Quantum correlations and mutual synchronization. *Phys. Rev. A* **85**, 052101 (2012).

34. Giorgi, G. L., Plastina, F., Francica, G. & Zambrini, R. Spontaneous synchronization and quantum correlation dynamics of open spin systems. *Phys. Rev. A* **88**, 042115 (2013).
35. Mari, A., Farace, A., Didier, N., Giovannetti, V. & Fazio, R. Measures of quantum synchronization in continuous variable systems. *Phys. Rev. Lett.* **111**, 103605 (2013).
36. Blatt, R. Delicate information. *Nature* **412**, 773 (2001).
37. Kwiat, P. G., Berglund, A. J., Altepeter, J. B. & White, A. G. Experimental verification of decoherence-free subspaces. *Science* **290**, 498–501 (2000).
38. Dicke, R. H. Coherence in spontaneous radiation processes. *Phys. Rev.* **93**, 99 (1954).
39. Palma, G., Suominen, K. & Ekert, A. Quantum computers and dissipation. *Proc. R. Soc. Lond. A* **452**, 567–584 (1996).
40. Raimond, J. M., Goy, P., Gross, M., Fabre, C. & Haroche, S. Statistics of millimeter-wave photons emitted by a Rydberg-Atom Maser: an experimental study of fluctuations in single-mode superradiance. *Phys. Rev. Lett.* **49**, 1924 (1982).
41. DeVoe, R. G. & Brewer, R. G. Observation of superradiant and subradiant spontaneous emission of two trapped ions. *Phys. Rev. Lett.* **76**, 2049 (1996).
42. Fink, J. M. et al. Dressed collective qubit states and the Tavis-Cummings model in circuit QED. *Phys. Rev. Lett.* **103**, 083601 (2009).
43. Mlynek, J. A., Abdumalikov, A. A., Eichler, C. & Wallraff, A. Observation of Dicke superradiance for two artificial atoms in a cavity with high decay rate. *Nat. Comms.* **5**, 5186 (2014).
44. Goban, A. et al. Superradiance for atoms trapped along a photonic crystal waveguide. *Phys. Rev. Lett.* **115**, 063601 (2015).
45. Braun, D. Creation of entanglement by interaction with a common heat bath. *Phys. Rev. Lett.* **89**, 277901 (2002).
46. Benatti, F., Floreanini, R. & Piani, M. Environment induced entanglement in markovian dissipative dynamics. *Phys. Rev. Lett.* **91**, 070402 (2003).
47. Zhao, Y. & Chen, G. H. Two oscillators in a dissipative bath. *Phys. A* **317**, 13–40 (2003).
48. Contreras-Pulido, L. D. & Aguado, R. Entanglement between charge qubits induced by a common dissipative environment. *Phys. Rev. B* **77**, 155420 (2008).
49. Zanardi, P. Dissipation and decoherence in a quantum register. *Phys. Rev. A* **57**, 3276 (1998).
50. Taylor, J. M. et al. Fault-tolerant architecture for quantum computation using electrically controlled semiconductor spins. *Nat. Phys.* **1**, 177–183 (2005).
51. Lidar, D. A., Chuang, I. L. & Whaley, K. B. Decoherence-free subspaces for quantum computation. *Phys. Rev. Lett.* **81**, 2594 (1998).
52. Bacon, D., Kempe, J., Lidar, D. A. & Whaley, K. B. Universal fault-tolerant quantum computation on decoherence-free subspaces. *Phys. Rev. Lett.* **85**, 1758 (2000).
53. Monz, T. et al. Realization of universal ion-trap quantum computation with decoherence-free qubits. *Phys. Rev. Lett.* **103**, 200503 (2009).
54. Wolf, A., De Chiara, G., Kajari, E., Lutz, E. & Morigi, G. Entangling two distant oscillators with a quantum reservoir. *EPL* **95**, 60008 (2011).
55. Roos, C. F., Chwalla, M., Kim, K., Riebe, M. & Blatt, R. Designer atoms for quantum metrology. *Nature* **443**, 316–319 (2006).
56. Levy, A. & Kosloff, R. The local approach to quantum transport may violate the second law of thermodynamics. *EPL* **107**, 20004 (2011).
57. Mitchison, M. T. & Plenio, M. B. Non-additive dissipation in open quantum networks out of equilibrium. *New J. Phys.* **20**, 033005 (2018).
58. Ferraro, D., Campisi, M., Andolina, G. M., Pellegrini, V. & Polini, M. High-power collective charging of a solid-state quantum battery. *Phys. Rev. Lett.* **120**, 117702 (2018).
59. Galve, F., Mandarino, A., Paris, M. G. A., Benedetti, C. & Zambrini, R. Microscopic description for the emergence of collective dissipation in extended quantum systems. *Sci. Reps.* **7**, 42050 (2017).
60. Gonzalez-Tudela, A. & Cirac, J. I. Quantum emitters in two-dimensional structured reservoirs in the nonperturbative regime. *Phys. Rev. Lett.* **119**, 143602 (2017).
61. Galve, F., Giorgi, G. L. & Zambrini, R. *Quantum correlations and synchronization measures in Lectures on General Quantum Correlations and their Applications*. (eds F. Fanchini, D. Soares Pinto, G. Adesso) 393–420 (Springer, Cham, 2017).
62. Bellomo, B., Giorgi, G. L., Palma, G. M. & Zambrini, R. Quantum synchronization as a local signature of super- and subradiance. *Phys. Rev. A* **95**, 043807 (2017).
63. Paz, J. P. & Roncaglia, A. J. Dynamics of the entanglement between two oscillators in the same environment. *Phys. Rev. Lett.* **100**, 220401 (2008).
64. Galve, F., Giorgi, G. L. & Zambrini, R. Entanglement dynamics of nonidentical oscillators under decohering environments. *Phys. Rev. A* **81**, 062117 (2010).
65. Watts, D. J. & Strogatz, S. H. Collective dynamics of ‘small-world’ networks. *Nature* **393**, 440–442 (1998).
66. Erdős, P. & Rényi, P. On random graphs. *Publ. Math. Debrecen* **6**, 290–297 (1959).
67. Bollobás, B. *Modern Graph Theory*. (Springer, New York, 1998).
68. Ringsmuth, A. K., Milburn, G. J. & Stace, T. M. Multiscale photosynthetic and biomimetic excitation energy transfer. *Nat. Phys.* **8**, 562–567 (2012).
69. Lidar, D. A. & Whaley, K. B. *Decoherence-Free Subspaces and Subsystems in Irreversible Quantum Dynamics* (eds Benatti, F. & Floreanini, R.) vol. 622, 83–120 (Springer Lecture Notes in Physics, Berlin, 2003).
70. Blume-Kohout, R., Khoo Ng, H., Poulin, D. & Viola, L. Information-preserving structures: A general framework for quantum zero-error information. *Phys. Rev. A* **82**, 062306 (2010).
71. An, N. B., Kim, J. & Kim, K. Nonperturbative analysis of entanglement dynamics and control for three qubits in a common lossy cavity. *Phys. Rev. A* **82**, 032316 (2010).
72. Zanardi, P. & Rasetti, M. Noiseless quantum codes. *Phys. Rev. Lett.* **79**, 3306 (1997).
73. Duan, L.-M. & Guo, G.-C. Preserving coherence in quantum computation by pairing quantum bits. *Phys. Rev. Lett.* **79**, 1953 (1997).
74. Manzano, G., Galve, F. & Zambrini, R. Avoiding dissipation in a system of three quantum harmonic oscillators. *Phys. Rev. A* **87**, 032114 (2013).
75. Prauzner-Bechcick, J. S. Two-mode squeezed vacuum state coupled to the common thermal reservoir. *J. Phys. A* **37**, 173 (2004).
76. Benedetti, C., Galve, F., Mandarino, A., Paris, M. G. A. & Zambrini, R. Minimal model for spontaneous quantum synchronization. *Phys. Rev. A* **94**, 052118 (2016).
77. Giorgi, G. L., Galve Fernando, F. & Zambrini, R. Probing the spectral density of a dissipative qubit via quantum synchronization. *Phys. Rev. A* **94**, 052121 (2016).
78. Cabot, A., Galve, F. & Zambrini, R. Dynamical and quantum effects of collective dissipation in optomechanical systems. *New J. Phys.* **19**, 113007 (2017).
79. Leykam, D., Andreanov, A. & Flach, S. Artificial flat band systems: from lattice models to experiments. *Adv. Phys. X* **66**, 1473052 (2018). and references therein.
80. Shutherland, B. Localization of electronic wave functions due to local topology. *Phys. Rev. B* **34**, 5208 (1986).
81. Bergman, D. L., Wu, C. & Balents, L. Band touching from real-space topology in frustrated hopping models. *Phys. Rev. B* **78**, 125104 (2008).
82. Nita, M., Ostahie, B. & Aldea, A. Spectral and transport properties of the two-dimensional Lieb lattice. *Phys. Rev. B* **87**, 125428 (2013).
83. Arzani, F., Fabre, C. & Treps, N. Versatile engineering of multimode squeezed states by optimizing the pump spectral profile in spontaneous parametric down-conversion. *Phys. Rev. A* **97**, 033808 (2018).
84. Underwood, D. L., Shanks, W. E., Koch, Jens & Houck, A. A. Low-disorder microwave cavity lattices for quantum simulation with photons. *Phys. Rev. A* **86**, 023837 (2012).
85. Lee, H., Cheng, Y.-C. & Fleming, G. R. Coherence dynamics in photosynthesis: protein protection of excitonic coherence. *Science* **316**, 1462–1465 (2007).
86. Collini, E. & Scholes, G. D. Coherent intrachain energy migration in a conjugated polymer at room temperature. *Science* **323**, 369–373 (2009).
87. Fassioli, F., Nazir, A. & Olaya-Castro, A. Quantum state tuning of energy transfer in a correlated environment. *J. Phys. Chem. Lett.* **1**, 2139–2143 (2010).
88. Wenlong Zhang et al. Depth-dependent decoherence caused by surface and external spins for NV centers in diamond. *Phys. Rev. B* **96**, 235443 (2017).
89. Scholak, T., de Melo, F., Wellens, T., Mintert, F. & Buchleitner, A. Efficient and coherent excitation transfer across disordered molecular networks. *Phys. Rev. E* **83**, 021912 (2011).



Open Access This article is licensed under a Creative Commons Attribution 4.0 International License, which permits use, sharing, adaptation, distribution and reproduction in any medium or format, as long as you give appropriate credit to the original author(s) and the source, provide a link to the Creative Commons license, and indicate if changes were made. The images or other third party material in this article are included in the article's Creative Commons license, unless indicated otherwise in a credit line to the material. If material is not included in the article's Creative Commons license and your intended use is not permitted by statutory regulation or exceeds the permitted use, you will need to obtain permission directly from the copyright holder. To view a copy of this license, visit <http://creativecommons.org/licenses/by/4.0/>.

© The Author(s) 2018